Seismic Performance of Large Brick Masonry Bearing Wall Strengthened by Post-Tension

H. Ousalem, Y. Miyauchi, M. Yamamoto, H. Kitajima & D. Ono
Takenaka Corporation, Japan

K. Murakami, H. Hayashi
Nikken Sekkei LTD, Japan

M. Kibayashi
The Building Center of Japan

SUMMARY:
Seismic performance and stability of a large brick masonry bearing wall strengthened with unbonded post-tensioning cables was examined through testing. The specimen was constructed referring to an existing building with 900 mm-thick walls in which holes were bored vertically from the top to the foundation to receive prestressing cables. The specimen was subjected to compression stress of 1.0 MPa and then a lateral loading was applied statically at its top. Loading was, first, applied in the out-of-plane direction inducing some damage to the element and then applied in the in-plane direction. Prestressing was effective where the damaged wall-specimen proved to be stable even at large lateral drifts. The predicted failure mode and assessed shear strengths of masonry using a simple approach were relatively close to test results. The assumed shear strength along mortar joint was found to be conservative when compared to the test results of nine small specimens that were subjected to different compression stresses ranging from 0.5 to 1.5 MPa.

Keywords: Unreinforced masonry wall, brick, post-tension, unbonded cable, seismic strengthening

1. INTRODUCTION

All over the world, buildings, bridges and aqueducts were, in the past, constructed using local materials and had as structural elements unreinforced masonry (URM) walls. These structural elements play a major role on the seismic response of the whole structure since they represent the basic resisting elements to horizontal seismic actions (Paulay and Priestley, 1992; FEMA, 2009). In seismically active regions, a large number of URM constructions have experienced heavy damage or collapsed during strong shakings (AIJ et al., 2001; Ousalem and Bechtoula, 2003; Decanini et al., 2004; FEMA, 2009; J.A.E.E. and A.I.J., 2012). Collapse of Christchurch Anglican cathedral tower, an architectural asset and a historic landmark in the city of Christchurch, New Zealand, which was built in the second half of the 19th century, during the 2011 earthquake is an expressive example. Many post-earthquake investigations and research studies revealed that such buildings are seismically vulnerable and should be considered for rehabilitation and retrofitting, particularly for those declared as important cultural and historical heritages (Cattanach et al., 2008; FEMA, 2009). Meanwhile, to proceed for retrofitting the assessment of the strength and deformation conditions of the existing structural elements becomes of relevance. Unfortunately, the scarce of experimental information on URM walls (material characteristics, structural element shapes, boundary conditions, etc.) as well as the actual conditions of URM constructions (oldness, implemented changes, location and environment, maintenance, etc.) makes the assessment task not simple to achieve neither before retrofit nor after.

While various technical methods have been practiced for seismic rehabilitation of URM structures (Qamaruddin , 1998; El-Gawady et al., 2004; Takiyama et al., 2009), there still exists little information or technical guidelines with which an engineer can judge the relative merits of these methods. Furthermore, there are no reliable analytical techniques to evaluate efficiently the seismic resistance of retrofitted masonry structures. Experimental results are constantly a reference at which designers turn to in order to provide vulnerable buildings with the most suitable retrofit technique.

However, because some buildings are very demanding in terms of seismic performance level to be achieved and/or because of some constraints like saving architectural aspects and preserving the existing space, some strengthening techniques cannot be implemented. Strengthening by post-tension is among few existing techniques that are very flexible, short time-consuming and suitable for historical buildings or buildings in which services and/or activities should not be disrupted. The structural performance of URM elements is enhanced by application of compression stresses, which eliminate, depending on external load conditions, entirely (serviceability conditions) or partially (ultimate conditions) tensile stresses in the masonry.

This paper reports two loading tests. First, in-plane monotonic loading shear tests were performed on nine post-tensioned small masonry specimens (wallettes), where basic characteristics of URM were investigated. Then, a lateral cyclic loading test was performed on a large post-tensioned brick masonry wall specimen. The seismic performance and stability of this wall was investigated in-plane and out-of-plane. All the experimental work was performed in the laboratories of Takenaka Corporation.

2. EXPERIMENTAL PROGRAM

The first experimental work consisted of investigating the evolution of shear strength of masonry when subjected to different compression stresses. Small specimens (Fig. 2.1) were one-wythe wallettes of seven brick layers each. They received compression stresses ranging from 0.5 to 1.5 MPa using external rods and were monotonically loaded in their plane using a three-point loading setup.

The second experimental investigation consisted of ensuring the stability of a large post-tensioned brick masonry wall beyond a certain level of damage. This wall received, vertically, a compression stress of 1.0 MPa using prestressing cables and then was laterally loaded at its top in a cantilever configuration using reversed loading cycles to simulate seismic effects. At first, loading was applied in the in-plane direction and then in the out-of-plane direction of the wall. This wall specimen (Fig. 2.2) was 2.6 m in height and 870 mm in thickness. It represented the lower part of 12m-tall and 900 mm-thick bearing walls of an existing historical building that will be strengthened by inserting unbonded prestressing cables through holes made by dry core drilling through the height of walls. To enhance the lateral capacity of the existing building, a constant compression stress of 1.0 MPa was intended to be applied on these walls. The compression level was decided based on actual compression strength of the existing masonry. Furthermore, to provide such walls with sufficient out-of-plane lateral capacity, prestressing cables were conceived as near as possible to the wall faces. Symmetrical configuration of excentered cables was adopted (170 mm eccentricity, Fig. 2.2). Vertically, prestressing cables were assumed to be uniformly distributed with about 1 m spacing along the length of walls.

2.1. Materials

The mechanical properties of bricks selected for constructing specimens were relatively different from those of the existing building due to the difficulty to find on market low quality bricks. The bricks used in specimens were slightly smaller in size and relatively higher in strength than the bricks of the existing building: average size of 210 mm x 85 mm x 50 mm in comparison to 224 mm x 108 mm x 61 mm, and compression strength of 33.6 MPa in comparison to 17.3 MPa. The compression strength of bricks was evaluated based on compression tests of prism samples (JIS R 1250, 2000; JIS A 5210, 1994).

As to joint mortar, one grade mortar having a 1:3.5 cement:coarse-sand proportion by weight and 65% water to cement ratio was used for all specimens. The average compression strength (JIS A 1108, 2006) and average tensile strength (JIS A 1113, 2006) of 100 mm x ϕ50 mm size mortar cylinders, after 28 days of curing, were 30.4 MPa and 0.32 MPa. The average tensile strength of existing mortar was 0.40 MPa.

Low relaxation high tensile grade steel rods (SPBR 1080/1230) of 11 mm diameter were selected for prestressing the wallettes. The average value of modulus of elasticity, guaranteed yield strength and guaranteed ultimate strength of rods were 200.0 GPa, 1080.0 MPa and 1230.0 MPa, respectively. Low relaxation high tensile grade steel prestressing cables (F170, 7xϕ15.2) of 45.6 mm diameter (970.9 mm^2 cross section) were selected for prestressing the large specimen. The average value of modulus of elasticity, guaranteed yield strength and guaranteed ultimate strength of cables were 196.8 GPa, 1428.0 MPa and 1680.0 MPa, respectively. Such large size of cables was selected to satisfy design load conditions in the out-of-plane direction.

2.2. Specimens

Nine small specimens (one-wythe wallettes) of seven brick layers each with 10-mm thick mortar joints were constructed (Fig. 2.1). The seven-layer length was decided to achieve three-point load shear tests. One large specimen of a rectangular shape was constructed as a full scale element reproducing the walls of an existing building. The specimen had four full-bricks in depth and was constructed using English bond, which is made up of alternating courses of stretchers and headers (Fig. 2.2). The brick layers were jointed by a 10-mm thick mortar. The specimen had a stiff reinforced concrete base.

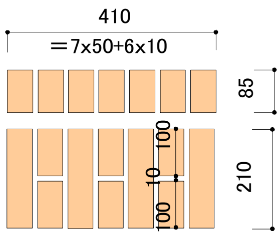

Figure 2.1. Outline of small specimens: Dimensions, brick arrangement, loading direction

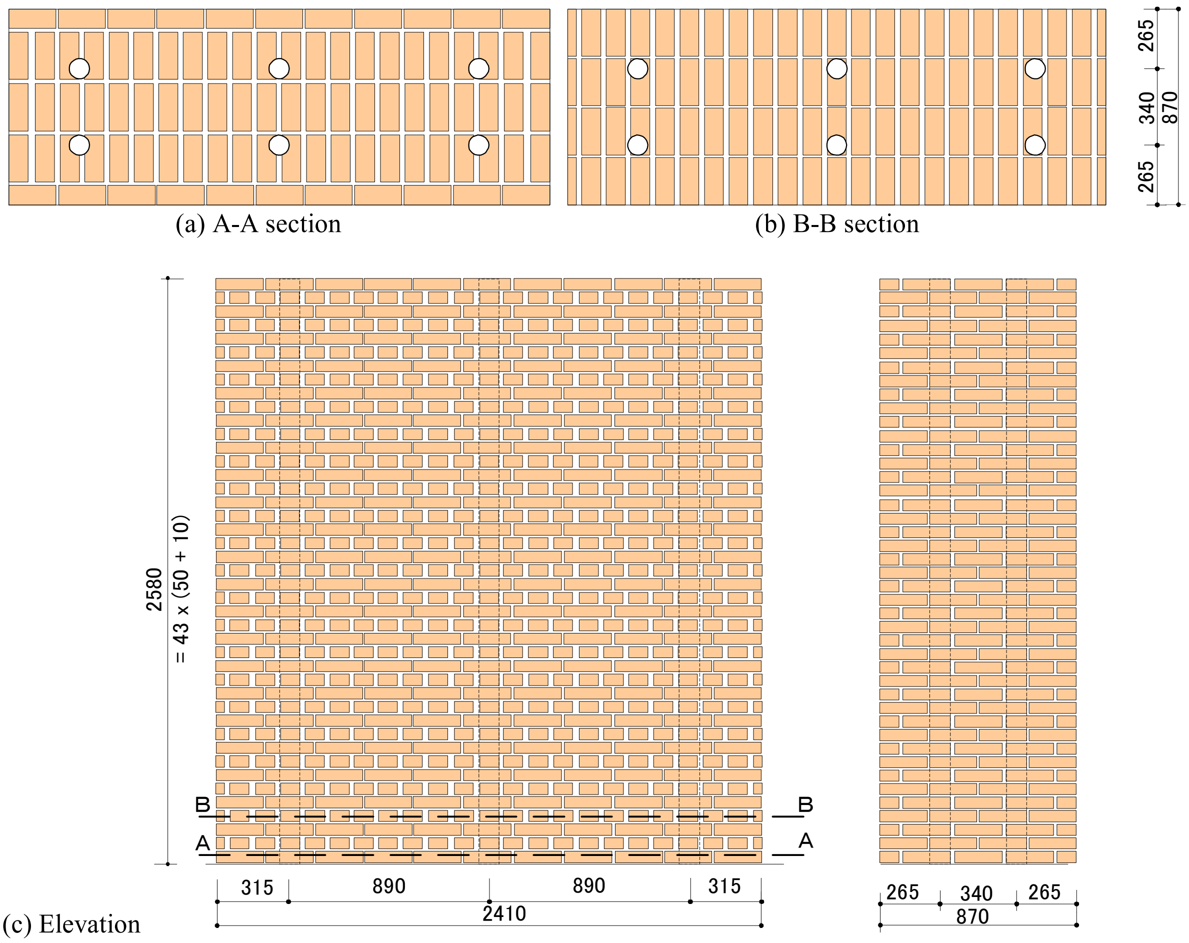

Figure 2.2. Outline of large specimen: Dimensions, brick arrangement in even layers (B-B section) and in odd layers (A-A section), drilled holes' location, lateral loading directions

2.3. Loading and Test Setup

After curing the specimens for about 40 days, prestressing was introduced and then testing was carried out. Table 2.1 lists the size of specimens and their corresponding compression levels.
The wallettes were prestressed just before testing using two 11 mm-diameter rods, installed externally. The vertical loading was applied monotonically till failure in a three-point loading configuration using a universal testing machine (Fig. 2.3.a). The whole test was carried out by force control. Deflection at the wallettes' mid-span was monitored by means of an LVDT installed below the lower surface of the specimens. Strains in the prestressing rods were measured by means of strain gauges.

Table 2.1. Size of Specimens and Prestressing Levels

Specimen	Width W (mm)	Length L (mm)	Height H (mm)	Number of prestressing elements n	Tension by prestressing element T (kN)	Masonry compression stress level σ (MPa)
MS-05*	85	410	210	2	4.46	0.5
MS-10*					8.93	1.0
MS-15*					13.39	1.5
ML-10	870	2410	2580	6	349.45	1.0

*: 3 samples for each case

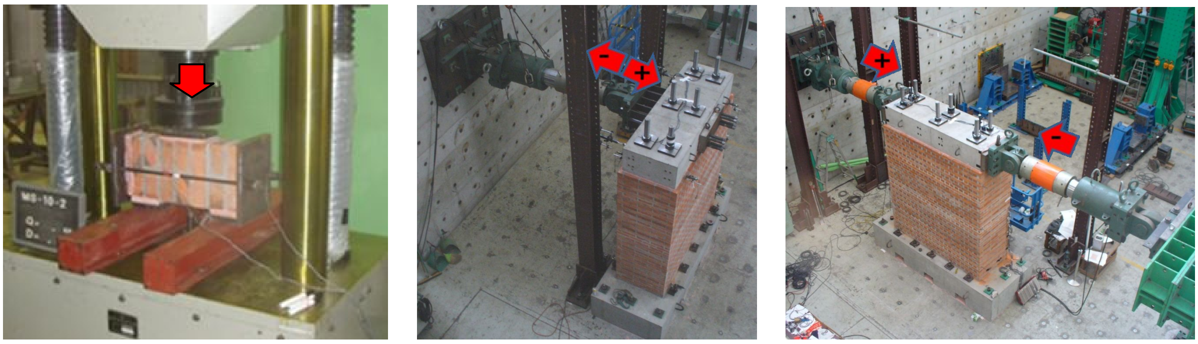

(a) Small specimen (b) Large specimen (in-plane) (c) Large specimen (out-of-plane)
Figure 2.3. Loading setup of specimens

Before applying lateral loading, the large specimen was prestressed using six 7xϕ15.2 cables installed into the wall-specimen through the drilled holes. A stiff reinforced concrete beam of 400 mm in height was used to distribute prestressing force vertically on the wall and to operate lateral loading in a cantilever configuration (Fig. 2.3b and Fig. 2.3c). Lateral cyclic-reversed loading with increasing amplitudes was applied using 2500/5000 kN hydraulic jacks. While only one jack acting in push-pull mode was used to apply lateral loading in the out-of-plane direction, two jacks acting in push-mode each were placed on opposite sides to apply lateral loading in the in-plane direction. The specimen was first loaded in the out-of-plane direction (Fig. 2.3.b) and after a certain level of damage it was loaded in the in-plane direction (Fig. 2.3.c). For both directions, loading was carried out under force control for the first eight cycles and then proceeded under displacement control till the end of testing. Two cycles were performed for every amplitude. The successive amplitudes in case of out-of-plane loading were Q=±50kN, ±100kN, ±150kN, ±300kN, for load control process followed by R=±1.0/1000, ±2.0/1000, ±3.3/1000, ±5.0/1000, ±7.5/1000 and ±10.0/1000, for displacement control process in terms of lateral drift ratio. The successive amplitudes in case of in-plane loading were Q=±150kN, ±300kN, ±450kN, ±600kN, followed by R=±1.0/1000, ±2.0/1000, ±3.3/1000, ±5.0/1000, ±7.5/1000 and ±10.0/1000. As to axial loading, except the dead loads of the concrete beam and wall and the prestressing force, no other vertical loads were applied on the specimen.
Deflections, slippage and shear deformations at different locations along walls' height were monitored by means of LVDTs installed on specimen's surface. Strains in the prestressing cables were measured by means of strain gauges installed on each cable. Hydraulic jacks were provided with load-cells.

2.4. Strength Assessment

A simplified approach for calculation of lateral strength of specimens was adopted in association to distinct common failure modes.
For shear strength assessment, calculations were based on the Coulomb criterion. The ultimate shear strengths of wallettes and large specimen were estimated using the following expression.

$$Q_s = (\tau_0 + \mu \sigma) A \tag{2.1}$$

where σ = compression stress (prestress), τ_0 = initial shear stress at zero compression stress (assumed 0.15 MPa), μ = friction coefficient (assumed 0.5 MPa) and A = specimen's cross-section.
For flexural strength assessment of the large specimen, focus was toward flexural cracking of joint mortar and crushing of masonry.
The lateral strength at first crack was calculated by balancing moments of the prestress load and lateral load, as given in the following expression. The tensile strength of mortar was neglected.

$$Q_c = \sigma A \frac{\sum_i l_i}{n(H + h_0)} \tag{2.2}$$

where σ = compression stress (prestress), A = wall's cross-section, l_i = lever-arm of the farthest prestressing cable i measured from rotation axis at the bottom of the wall, n = total number of prestressing cables, H = height of the masonry wall, and h_0 = half of the section-height of the loading beam (herein 200 mm).
The lateral strength at crushing of masonry was calculated through an iterative procedure to find the neutral axis position based on the equivalent rectangular compression stress block. The effective height of the compression stress block was assumed 80% of the neutral axis depth. The strength reduction factor of masonry was taken as 0.75. The compression strength, Young modulus and ultimate strain of masonry were assumed to be 15 MPa, 10000 MPa and 0.0015, respectively. First, strains of the unbounded cables were evaluated according to the assumed displacement at the top of the wall, and then the curvature and the position of the neutral axis at the base of the wall were calculated. Finally, equilibrium of internal forces developed along the wall section was checked, moments (M_u) of all these forces were taken about the neutral axis and lateral strength at crushing was obtained.

$$Q_{mu} = \frac{M_u}{H + h_0} \tag{2.3}$$

3. TEST RESULTS AND DISCUSSION

Failure modes, cracks development, deformation proportions and force-displacement diagrams obtained from monotonic tests of wallettes and cyclic tests of large specimen were necessary to evaluate the seismic performance of prestressed masonry. Test results are illustrated in photos and figures and summarized in tables. The later include assessed strengths of specimens based on the assumed characteristics of the masonry using the equations presented previously in Section 2.4.

3.1. Small Specimens (Wallettes)

Under monotonic shear loading, specimens experienced a same failure mode, though subjected to different compression stresses. A sudden crack appeared, generally, at the interface of the mortar joint and brick units as shown in Fig. 3.1. Beyond the first cracking, shear strength kept increasing due to bending effect which induced an additional elongation of prestressing rods. Therefore, the load level at cracking and its corresponding average vertical displacement δ_v were higher for specimens with higher compression stress. Discrepancies in the results of each series were noticed. This may be explained by some variations in materials' characteristics.

Table 3.1 summarizes test results of wallettes at first crack as well as assessed strengths. The later, based on the shear stress at zero compression stress τ_0 =0.15 MPa and the friction μ =0.5, were about half of test results. This suggests that the assumed values of shear stress and friction particularly were conservative. This conclusion was confirmed by other works carried out by Ousalem et al. (2010b) on various sizes of brick masonry specimens. Fig. 3.2 relates shear stress results to compression stresses of the tested wallettes. The figure also includes other test results obtained by the same authors (in the figure, S, M and L refer to small, middle and large size specimens, respectively).

Figure 3.1. Common failure shape of wallettes

Table 3.1. Assessed Strengths and Test Results of Wallettes

Specimen	σ (MPa)	$^*Q_{s,\ calculation}$ (kN)	$Q_{s,\ test}$ (kN)	δ_v (mm)	τ (MPa)
MS-05	0.5	0.40	11.69	0.73	0.66
			12.41	0.59	0.70
			13.69	0.40	0.77
MS-10	1.0	0.65	17.80	0.49	1.00
			21.38	0.67	1.20
			21.19	0.76	1.19
MS-15#	1.5	0.90	36.73	0.70	2.06
			34.1	0.93	1.91

*: Eq.(2.1), #: third specimen experienced cracks before testing

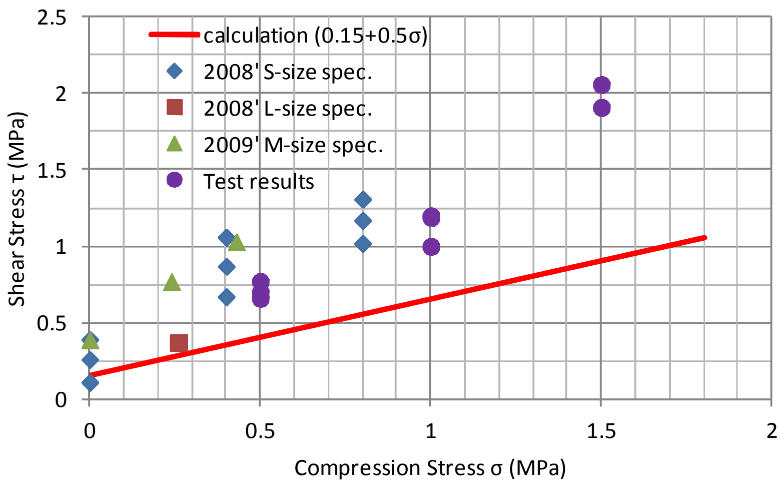

Figure 3.2. Shear stress-compression stress relationship

3.2. Large Specimen

The large specimen was loaded, first, in the out-of-plane lateral direction then after a certain level of damage the direction of lateral loading was changed and the specimen was loaded in the in-plane direction.
Initially, under the first stages of both out-of-plane and in-plane loadings, specimen's cross section was under compressive stresses and therefore no cracks were observed anywhere. First cracks appeared at the bed joint or at the lower two first layer joint when the applied stress condition due to lateral loading exceeded the effective normal stress (prestressing and tensile strength of mortar). Subsequent lateral loading lengthened flexural cracks and gradually induced full rocking in case of out-of-plane loading and combined rocking/sliding in case of in-plane loading, increased tensile stresses in prestressing cables and brought in very high compressive stresses at the bottom edges of the specimen, resulting in some crushing. Cracks and damage concentrated only at the bottom of the wall. The large specimen showed a high seismic performance for both loading directions. The assessed strength values predicted that flexure failure would prevail under the out-of-plane loading and shear/flexure failure would prevail under the in-plane loading. Table 3.2 summarizes the test results and assessed strength values expressed by the equations in Section 2.4.

Table 3.2. Test Results and Assessed Strengths of Large Specimen

Loading Direction		Out-of -Plane	In-Plane
Assessed Strength	First crack $^{\#}Q_c$ (kN)	228.5	528
	Crushing $^{\$}Q_{mu}$ (kN)	511.5	1588
	Shear $^{\&}Q_s$ (kN)	1363	1363
Failure Mode (Prediction)		Flexure	Shear/Flexure
Stiffness (Test)	K (kN/mm)	153	554
First Flexural Crack (Test)	Shear Strength Q_c (kN)	265.8 (-198.8)	520^* (-550^*)
	Drift Ratio R_c (1/1000)	0.71 (-0.55)	0.31 (-0.34)
	Cable tension: T_{max} ,T_{min} (kN)	367, 352 (364, 353)	367, 343 (367, 343)
Bottom edge Crushing (Test)	Shear Strength Q_{mu} (kN)	496.9 (-429.9)	1398.4 (-1352.1)
	Drift Ratio R_{mu} (1/1000)	7.53 (-7.48)	3.30 (-3.31)
	Cable tension: T_{max} ,T_{min} (kN)	554, 404 (544, 400)	643, 330 (608, 325)
Failure Mode (Test)		Rocking/Crushing	Rocking/Crushing/Sliding
Shear deformation		Negligible (below 0.3mm)	Max 0.64mm at R=-10/1000
Slippage		Negligible (below 0.3mm)	Max 6.72mm at R=+10/1000

Note: $^{\#}$: Eq.(2.2); $^{\$}$: Eq.(2.3); $^{\&}$: Eq.(2.1); Values in parentheses refer to test results in the negative loading direction; Cables' tension values are simultaneous results of extreme rods located at opposite sides in the direction of loading; *: value relative to the opening of the existing crack of previous out-of-plane loading test

The tested specimen showed, under the out-of-plane loading, a self-centering behavior as illustrated by the remarkable S shape of the hysteresis loops in Fig. 3.3. The specimen did not dissipate energy. It exhibited a significant nonlinear response with no strength degradation. All horizontal cracks that developed at the bed mortar joint of the wall's bottom closed or their width became insignificant after unloading the specimen from cycles' peaks as well as at the end of the loading stage. The specimen underwent a slight damage as illustrated in Fig. 3.4.
The in-plane cyclic behavior was governed by flexural response till the end of loading where slippage was almost inexistent. Displacement due to shear deformation was very negligible (less than 0.3mm at maximum). The first crack appeared at the bed joint at almost the same lateral drift ratio (0.07%) in the positive and negative directions. Since then, wall stiffness decreased and strains in cables experienced an important change. They increased with increasing drift ratio. After a relatively large drift (0.75%), crushing occurred at the extreme compressed edges of the specimen but was not severe without any sign of strength degradation until the end of testing, which was soon after crushing of masonry. The test crack load level and crushing load level were very close to the strength evaluated by the simple approach of Section 2.4 for flexural behavior case.

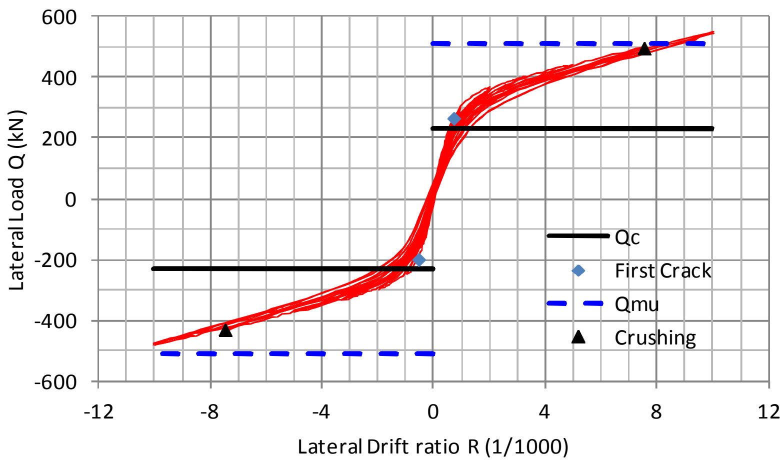

Figure 3.3. Lateral force-lateral drift ratio diagram under out-of-plane loading

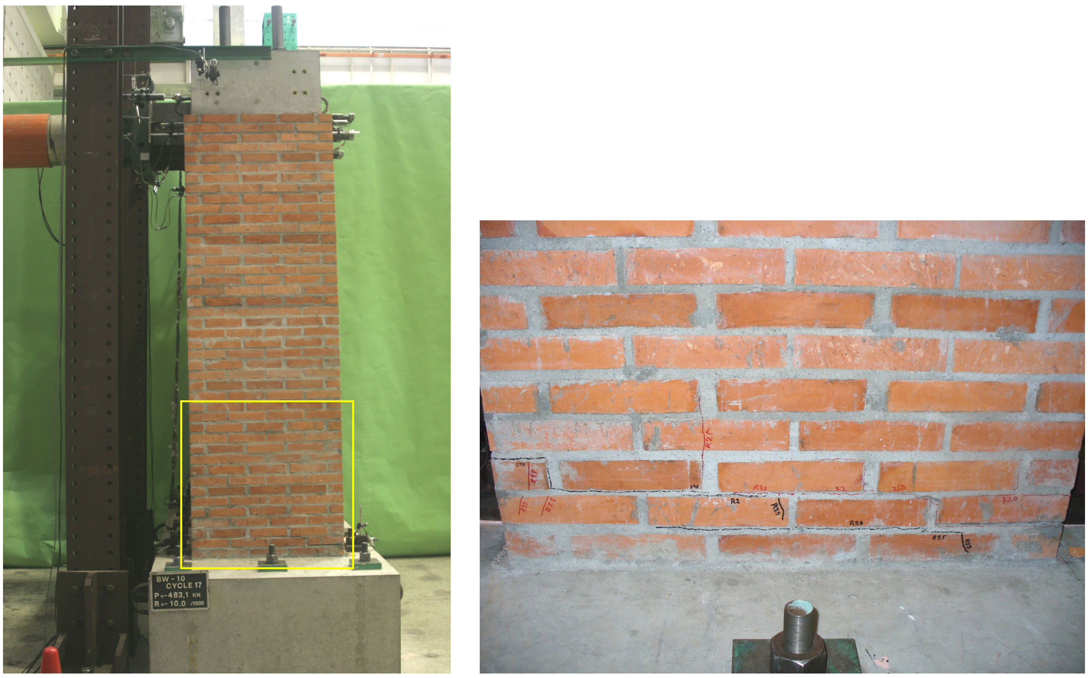

Figure 3.4. Deformation and damage condition of specimen at drift ratio -1% under out-of-plane loading

Although the specimen underwent some damage under the out-of-plane loading, the in-plane cyclic response was mainly governed by flexure where the specimen exhibited a significant nonlinear response with no strength degradation and showed a self-centering behavior until the drift ratio of 0.2%, as illustrated in Fig. 3.5. Since that level, the specimen started to dissipate energy due to slippage which was smooth and not severe. At the end of loading, negligible displacement due to shear deformation was noticed and slippage reached 6.7mm. First crack load level at the bed joint was determined when cracks at the bottom of the specimen from the previous test opened at almost the same lateral drift ratio (0.03%) in the positive and negative directions. Since then, wall stiffness decreased and strains in cables increased consistently with increasing drift ratio. At the drift ratio of 0.33%, crushing occurred at the extreme compressed edges of the specimen. Although crushing was relatively severe, no sign of strength degradation was observed until the end of testing and the specimen remained stable with a slightly visible residual displacement at the bottom of the wall (Fig. 3.6). The test crack load level and the crushing load level were, respectively, very close and relatively close to the strengths evaluated by the simple approach of Section 2.4.

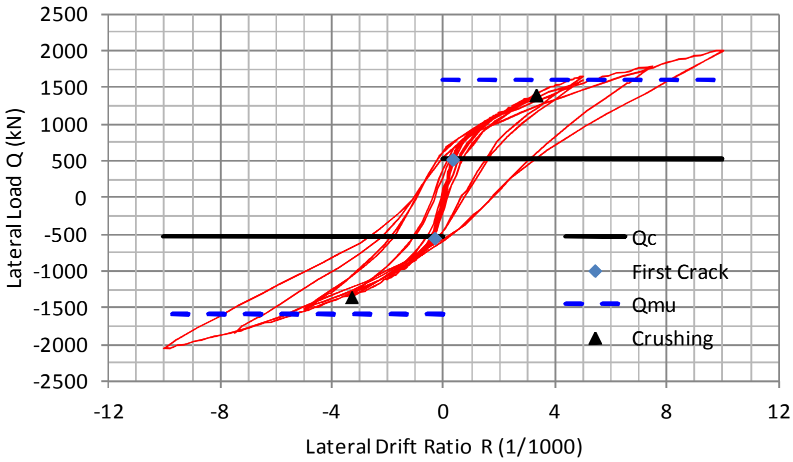

Figure 3.5. Lateral force-lateral drift ratio diagram under in-plane loading

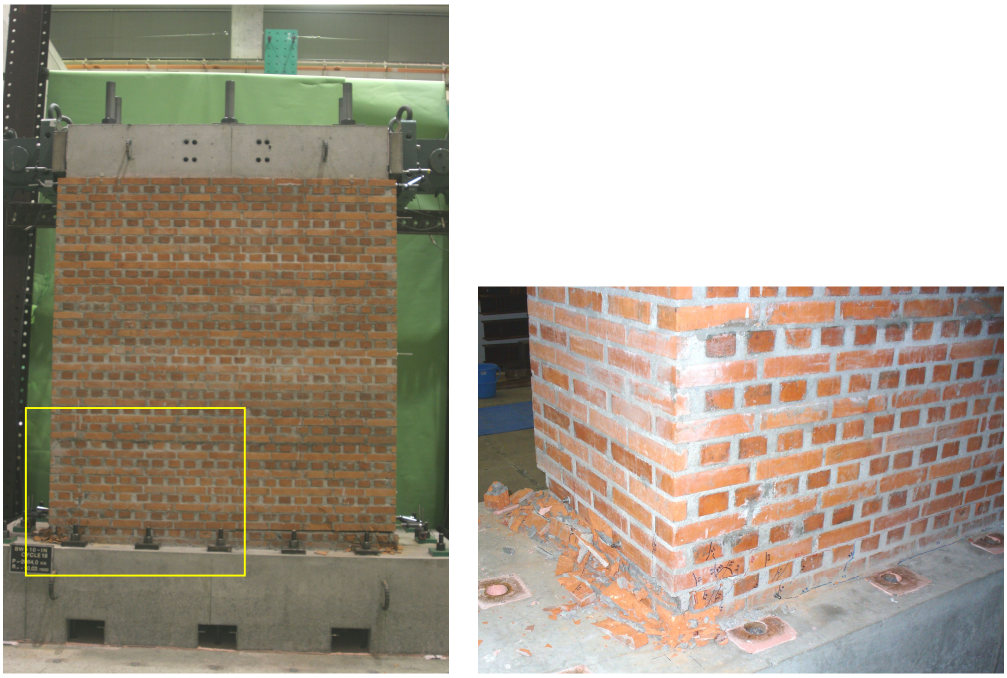

Figure 3.6. Deformation and damage condition of specimen at drift ratio -1% under in-plane loading

4. CONCLUSION

Nine similar wallettes subjected to different compression stress levels and one post-tensioned large brick masonry wall were tested to investigate some basic characteristics of brick masonry, evaluate the effectiveness of prestressing on the seismic performance of large masonry walls and ensure the stability of such walls beyond a certain level of damage. Prestressing proved to be very effective where shear stress of masonry increased with increasing compression stress. However, the basic characteristics of masonry through wallettes' testing were found to be higher than the assumed ones, particularly the friction. As to the structural seismic performance of masonry walls, the strengthened large specimen showed a flexural behavior and was stable till the end of loading without noticeable strength degradation even at relatively large lateral drifts. Similarly to other large walls of different aspect ratios and shapes (Ousalem et al., 2010a; 2010b), the assessed strengths based on a simple approach seems suitable for masonry walls and were relatively close to test results.

REFERENCES

A.I.J., J.S.C.E. and J.G.S. (2001). Report on the Damage Investigation of the 1999 Kocaeli Earthquake in Turkey, Architecture Institute of Japan, Japan

Cattanach, A.G., Alley, G.W. and Thornton, A.W. (2008). Appropriatness of Seismic Strengthening Interventions in Heritage Buildings: A Framework for Appraisal. *2008 New-Zealnd Earthquake Engineering Conference*. Paper 30.

Decanini, L., De Sortis, A., Goretti, A., Langenbach, R., Mollaioli, F. and Rasulo, A. (2004). Performance of Masonry Building during the 2002 Molise, Italy, Earthquake, *Earthquake Spectra* **20:S1**,191-220.

El-Gawady, M., Lestuzzi, P. and Badoux, M. (2004). A Review of Conventional Seismic Retrofitting Techniques for URM. *Thirteenth International Brick and Block Masonry Conference*. **Vol II**, 381-390

FEMA, (2009). Unreinforced Masonry Buildings and Earthquakes: Developing Successful Risk Reduction Programs, FEMA P-774, U.S.A.

J.A.E.E. and A.I.J. (2012). Report of the Joint mission of Japan Association for Earthquake Engineering and Architectural Institute of Japan to the areas affected by the Feb. 22, 2011 Christchurch Earthquake, Japan (Draft, to be published)

JIS A 1108, (2006). Method of Test for Compressive Strength of Concrete, Japanese Standards Association, Japan (in Japanese)

JIS A 1113, (2006). Method of Test for Splitting Tensile Strength of Concrete, Japanese Standards Association, Japan (in Japanese)

JIS A 5210, (1994). Ceramic Masonry Units for Buildings, Japanese Standards Association, Japan (in Japanese)

JIS R 1250, (2000). Common Bricks and Facing Bricks, Japanese Standards Association, Japan (in Japanese)

Ousalem, H. and Bechtoula, H. (2003). Report on the Damage Investigation and Post-Seismic Campaign of the 2003 Zemmouri Earthquake in Algeria, Ohbunsha Press, Japan

Ousalem, H., Miyauchi, Y., Yamamoto, M., Kibayashi, M., (2010a). Experimental Investigation of Post-Tensioned Brick Masonry Bearing walls. *Fourteenth European Conference on Earthquake Engineering, Ohrid, Republic of Macedonia*. Paper 359

Ousalem, H., Miyauchi, Y., Yamamoto, M., Kibayashi, M., Nezu,S. and Higashi, K. (2010b). In-Plane Loading Tests of Brick Masonry Bearing Walls Seismically Strengthened by Post-Tension. *Ninth Japan-China Joint Conference on Structural Engineering, Tokyo, Japan*. 765-774

Paulay, T. and Priestley, M.J.N. (1992). Seismic Design of Reinforced Concrete and Masonry Buildings, John Wiley & Sons, Inc., U.S.A.

Qamaruddin, M. (1998). A State-of-the-Art Review of Seismic Isolation Scheme for Masonry Buildings, *ISET Journal of Earthquake Technology*, **35:4**, paper No.376, 77-93.

Takiyama, N., Nagae, T., Maeda, H., Kitamura, M., Yoshida, N., Araki, Y. (2009). Seismic Retrofit of Historic Masonry Constructions by Inserting Stainless Pins : Cyclic Out-of-Plane Flexural Experiments of Reinforced Brick Walls, Part I, *Journal of Structural and Construction Engineering*, *A.I.J*, **74:635**, 167-176 (in Japanese)